Communication

Effect of Physicochemical Properties of Slag and Flux on the Removal Rate of Oxide Inclusion from Molten Steel

JUN SEOK PARK and JOO HYUN PARK

The slag-metal reaction experiments were carried out using a high-frequency induction furnace to confirm the effect of slag composition on the removal rate of inclusions in molten steel through the CaO-based slags. The apparent rate constant of oxygen removal (k_O) was obtained as a function of slag composition. It increased with increasing basicity, and the content of MgO and CaF_2, whereas it decreased by increasing the content of Al_2O_3 in the slag. The removal rate of inclusions was strongly affected not only by the driving force of the chemical dissolution but also by the viscosity of the slags and fluxes.

Non-metallic inclusions in the steel cause the deterioration of the mechanical properties as well as severe problems during steelmaking and casting processes.[1–3] For above reasons, the cleanliness of the steel has been important and lots of studies about not only the modification of inclusions but also the removal of the inclusions using slags and fluxes have been reported for several decades. Accordingly, the studies for the mechanism of inclusion removal in the steel melt have been carried out by many researchers.[4–16] Some of them employed the rotating rod method for measuring alumina dissolution rate in the slag,[4–6] the others recently observed the in-situ dissolution phenomena of the inclusions into the slag using a confocal scanning laser microscope (CSLM).[7–14] A direct measurement of the removal rate of inclusions in industrial practice has also been reported.[15,16]

JUN SEOK PARK, formerly Graduate Student, is now Researcher with the Ultimate Manufacturing Technology Group, Korea Institute of Industrial Technology (KITECH), Daegu 711-883, Korea. JOO HYUN PARK, Professor, is with the Department of Materials Engineering, Hanyang University, Ansan 426-791, Korea. Contact e-mail: basicity@hanyang.ac.kr.

Sandhage and Yurek reported that sapphire is indirectly dissolved into the CaO-MgO-Al_2O_3-SiO_2 melts and that $CaO \cdot 6Al_2O_3$ (CA6) and/or $MgO \cdot Al_2O_3$ (MA) phases were formed at the interface between sapphire and silicate melts during dissolution of sapphire.[4,5] They also found that MA phase inhibits the dissolution of the sapphire. Choi et al.[6] measured the dissolution rate of alumina rod into the CaO-SiO_2-Al_2O_3 melts at 1873 K (1600 °C) and constructed the iso-dissolution rate contours. They concluded that the dissolution of alumina into the CaO-SiO_2-Al_2O_3 melts is controlled by mass transfer in the slag phase. It was also found that $CaO \cdot 2Al_2O_3$ (CA2) or CA6 is formed at the interface between melts and alumina depending on the slag composition, which is similar to the findings of Sandhage and Yurek.

Sridhar et al.[7–10] studied the dissolution of alumina particles in the CaO-Al_2O_3-SiO_2-MgO slags and found that alumina was directly dissolved into the MgO-free slags, while the reaction layer, MA, was formed in MgO-containing slags during the dissolution process. For the dissolution of Al_2O_3 and MgO in the silica-free CaO-Al_2O_3-MgO slag, it was reported that Al_2O_3 dissolution was explained by a diffusion-controlled dissolution process, whereas MgO dissolution was controlled by chemical reaction kinetics.[8] More recently, they reported that the dissolution time of inclusions is inversely proportional to the ratio of driving force (concentration difference, ΔC) to slag viscosity (η), viz. $\Delta C/\eta$ ratio.[9] Although above-mentioned studies attributed to understand the mechanism of the dissolution of inclusion in the slag, they are partly restricted to the industrial applications since many of them indirectly estimated the inclusion removal process.

A few studies reported the change of the total oxygen in the steel melt during steelmaking process by employing the industrial results.[15,16] However, because they just estimated the difference in oxygen content before and after refining process in the viewpoint of the removal efficiency of inclusions,[15,16] it is difficult to quantitatively estimate the removal rate of inclusions. Therefore, in the present study, we carried out the slag-metal reaction experiments using a high-frequency induction furnace in order to estimate the effect of slag composition on the removal rate of inclusions in molten steel through the CaO-based slags. This methodology has an advantage that the change of the total oxygen in the steel melt can be directly obtained by sampling in a very short time interval.[17–20]

The Fe-0.2($\pm$0.02) mass pct O alloy was prepared in a fused MgO crucible (OD: 60 mm, ID: 52 mm, H: 120 mm) by blowing oxygen gas into the iron melt during 20 minutes using an induction furnace. The slag was pre-melted in a graphite crucible (OD: 50 mm, ID: 44 mm, H: 88 mm) during 2 hours in an electric resistance furnace under purified Ar atmosphere. Some slags, disintegrated into fine powders due to high basicity,

Table I. Initial Composition of Slags in Present Experiments

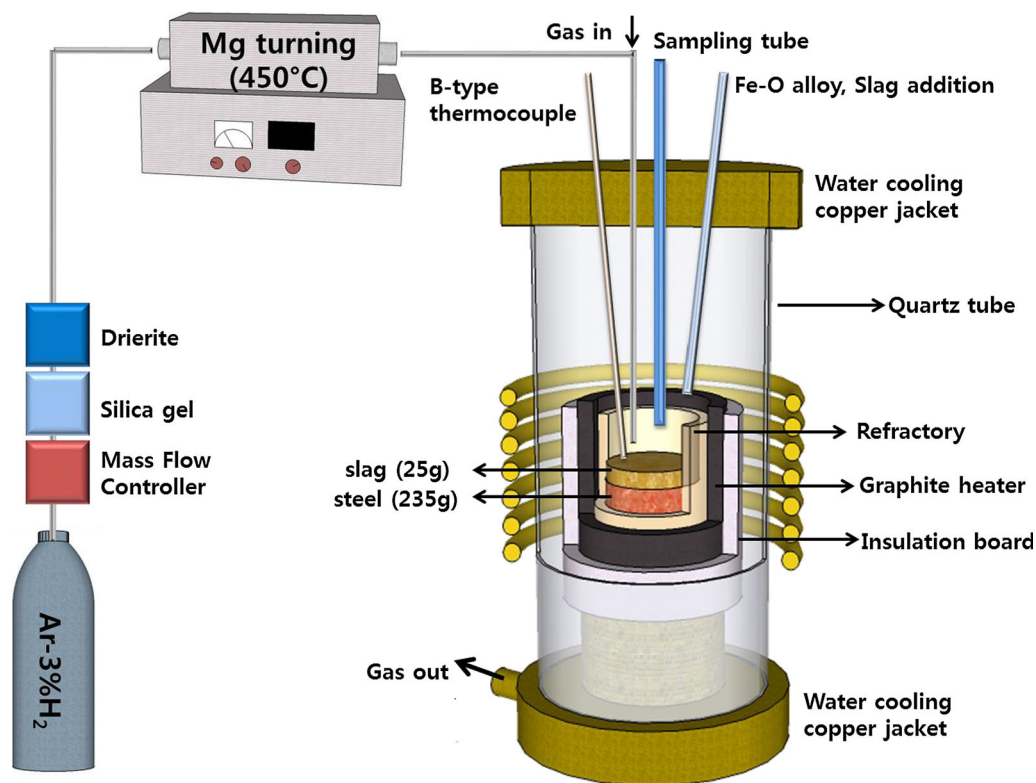| Exp. Series	Initial Slag Composition (Mass Pct)				
	CaO	CaF$_2$	SiO$_2$	Al$_2$O$_3$	MgO
#1	23.0	20.0	47.0	5.0	5.0
#2	35.0	20.0	35.0	5.0	5.0
#3	42.0	20.0	28.0	5.0	5.0
#4	47.0	20.0	23.0	5.0	5.0
#5	50.0	20.0	25.0	0.0	5.0
#6	43.0	20.0	22.0	10.0	5.0
#7	40.0	20.0	20.0	15.0	5.0
#8	50.0	20.0	25.0	5.0	0.0
#9	43.0	20.0	22.0	5.0	10.0
#10	40.0	20.0	20.0	5.0	15.0
#11	53.0	10.0	27.0	5.0	5.0
#12	40.0	30.0	20.0	5.0	5.0

Fig. 1—Schematic diagram of the experimental apparatus.

were pelletized in order to accurately add to melt surface. The slag composition is shown in Table I. The schematic diagram of the experimental apparatus is given in Figure 1.[17–20]

After temperature reached at 1903 K (1630 °C), Fe-0.2 pct O alloy (65 g) was added into the Fe-1.5Mn-0.4Si-0.5Cr (mass pct) melt (235 g) under an inert atmosphere to control the initial oxygen content and then the slag (25 g) was added when temperature was recovered to 1873 K (1600 °C). Temperature was controlled by B-type thermocouple covered by alumina sheath. After slag was added (time = 0), suction sampling was performed at 1, 3, 5, 10, 30, and 60 minutes and then the samples were directly quenched by dipping them into brine. The rod-shaped samples were obtained using a quartz suction sampler having an inner diameter of 4 mm from the position of the center of the melt. The samples were cut and polished to cylinder and the weight of each sample was about 5 g. Each sample of 2.5 gram was used in analysis of total oxygen using a combustion analyzer and the other was used in analysis of inclusion composition. The content of total oxygen was analyzed by combustion analyzer after very careful ultrasonic cleaning and preparation
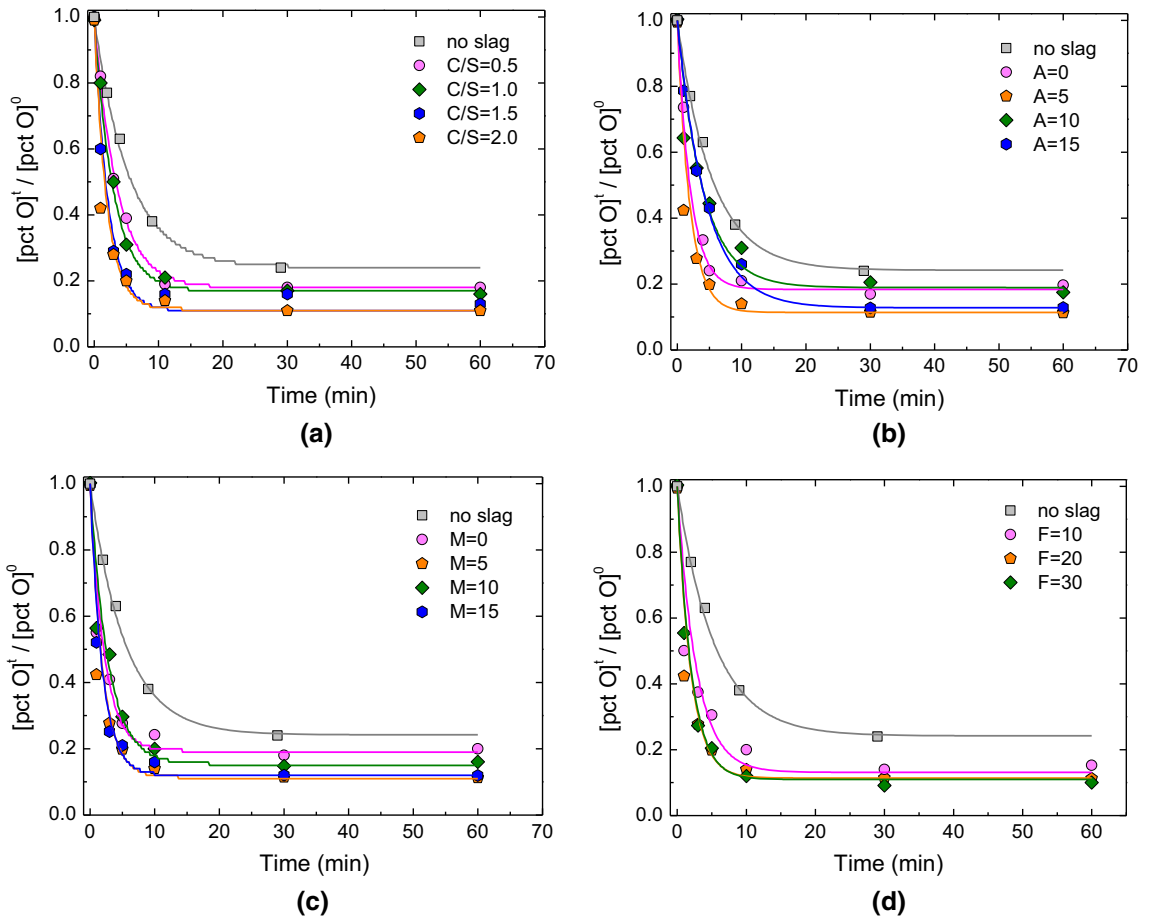
Fig. 2—Content of total oxygen (normalized) in the melt as a function of time at different (*a*) CaO/SiO$_2$ ratios, (*b*) Al$_2$O$_3$ contents, (*c*) MgO contents, and (*d*) CaF$_2$ contents in the slag at 1873 K (1600 °C).
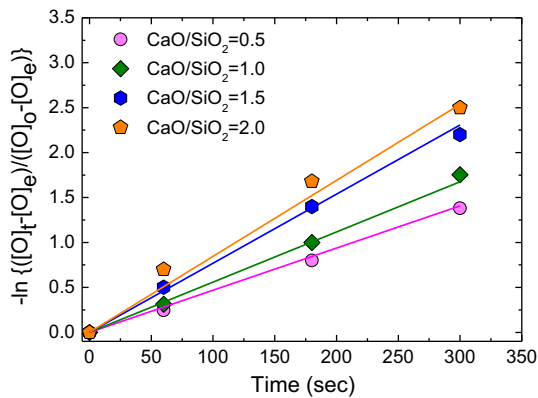

Fig. 3—Kinetic plot for estimating the apparent rate constant of inclusion removal from molten steel at 1873 K (1600 °C).

procedure. The sample for inclusion analysis was mounted and polished in order to observe the composition of the inclusions in the samples. The composition of the inclusions was analyzed using scanning electron microscopy coupled with energy-dispersive spectrometer (SEM-EDS, JSM-7800, JEOL). The slag composition was analyzed by X-ray fluorescence spectrometry (XRF, S4 explorer, Bruker).

The normalized total oxygen content in the melt decreases with reaction time, since the inclusions in the melt were removed by slag phase as shown in Figure 2. Here, the decrease of the total oxygen content in the melt is assumed to the decrease of the inclusions in the melt because dissolved oxygen in the melt immediately decreases after addition of deoxidizer.[21,22] In case of all experiments using slag phase, the oxygen content is lower than that in the absence of slag. The content of total oxygen in the melt reached equilibrium after 10 minutes. Accordingly, it can be assumed that the content of oxygen at equilibrium is the average value of the oxygen content at 30 and 60 minutes.

If the first-order reaction for oxygen removal reaction was assumed, the content of oxygen with reaction time can be written as shown in Eq. [1].

$$-\frac{d[pctO]_t}{dt} = k_O\left([pct\ O]_t - [pct\ O]_e\right) \qquad [1]$$

$$-\ln\left(\frac{[pctO]_t - [pctO]_e}{[pct\ O]_o - [pct\ O]_e}\right) = k_O t, \qquad [2]$$

where [pct O]$_t$ is the content of total oxygen in the melt at time t, [pct O]$_e$ is the content of total oxygen at equilibrium, k_O is an apparent rate constant of

Table II. Apparent Rate Constant of Inclusion Removal in conjunction with Chemical Driving Force of Alumina Dissolution and Viscosity of Slags

Exp. Series	ΔC (Mass Pct)	Viscosity at 1873 K (1600 °C) (dPa.s)	k_O ($\times 10^2$)
#1	25.7	2.20	0.469
#2	35.2	0.92	0.559
#3	39.4	0.64	0.769
#4	39.7	0.53	0.846
#5	46.1	0.48	0.810
#6	38.8	0.58	0.420
#7	33.6	0.64	0.372
#8	40.8	0.55	0.766
#9	46.1	0.51	0.594
#10	43.2	0.49	0.884
#11	40.5	0.61	0.606
#12	47.5	0.45	0.811
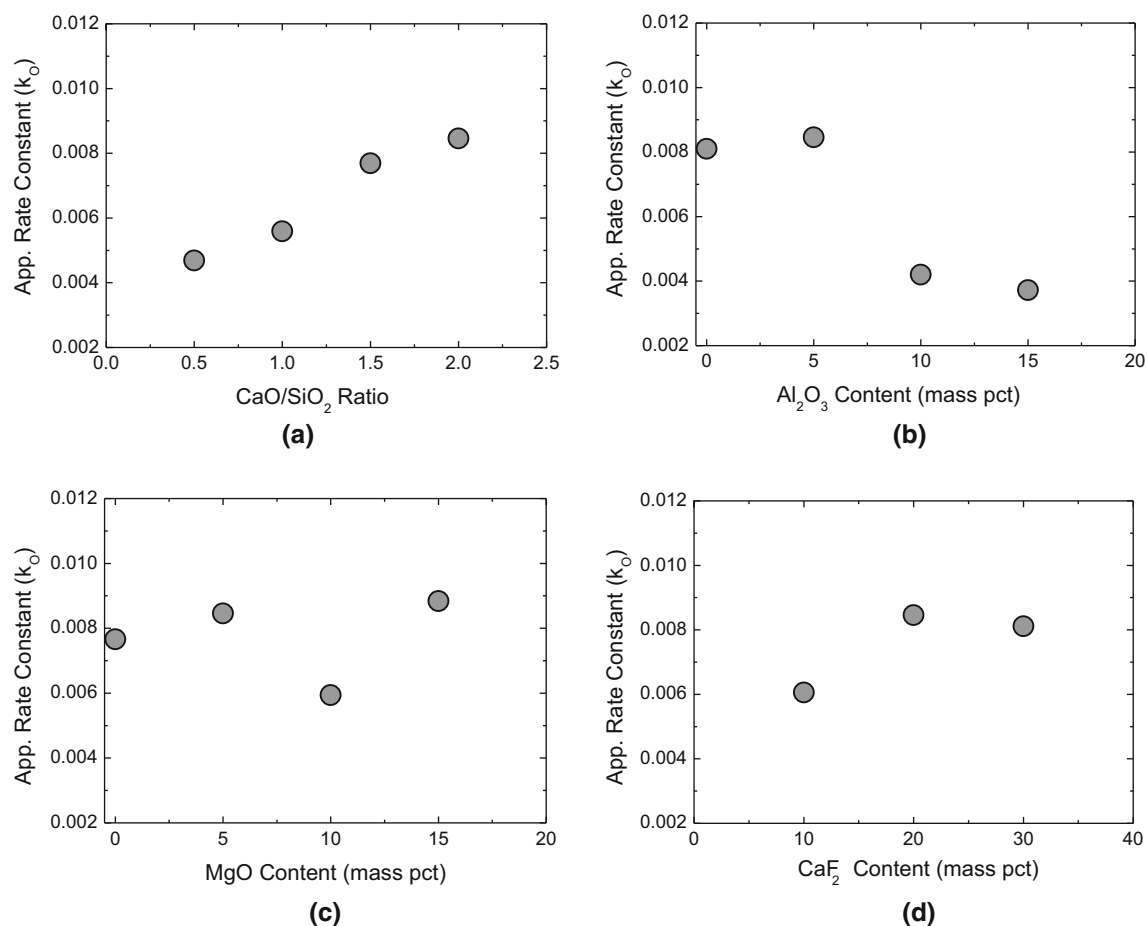
Fig. 4—Effect of (*a*) CaO/SiO$_2$ ratio, (*b*) Al$_2$O$_3$ content, (*c*) MgO content, and (*d*) CaF$_2$ content in the slag on the apparent rate constant of inclusion removal at 1873 K (1600 °C).

inclusions removal (s^{-1}), and [pct O]$_o$ is the initial content of total oxygen. Since the content of total oxygen in the melt reaches at an equilibrium after about 10 minutes, k_O was calculated by employing a linear regression analysis as shown in Figure 3, for example. The apparent rate constant of inclusion removal through various slags is listed in Table II. In Table II, the ΔC represents a difference in Al$_2$O$_3$ content between initial slag and final composition based on the

fact that the inclusions were mainly alumina, which will be discussed later. The viscosity of slag was calculated using FactSage^{TM}7.0 software. The application of these two physicochemical parameters will be discussed later (in Eq. [3]).

The effects of the CaO/SiO$_2$ ratio, and the content of Al$_2$O$_3$, MgO and CaF$_2$ on the apparent rate constant of inclusion removal are shown in Figure 4. Increase in the basicity (CaO/SiO$_2$) of slag causes an increase in the
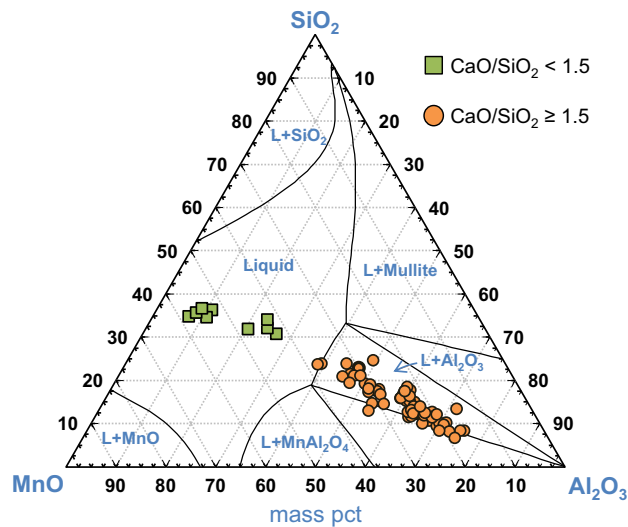
Fig. 5—Computed phase diagram of the MnO-Al_2O_3-SiO_2 system at 1873 K (1600 °C) and $p(O_2) = 10^{-13}$ atm. Solid marks represent the composition of the inclusions in steel samples.
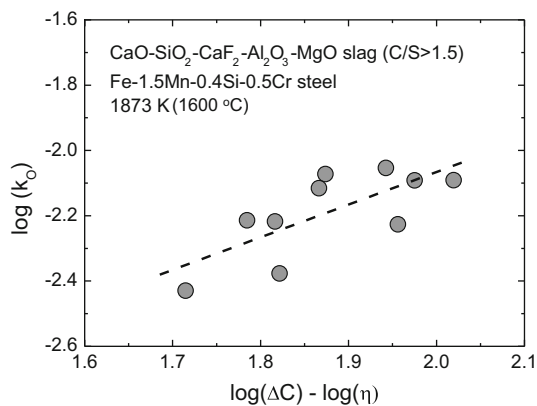

Fig. 6—Relationship between the apparent rate constant of inclusion removal reaction and the slag parameter including the driving force of the chemical dissolution of Al_2O_3 and the viscosity of the slag.

apparent rate constant under the present experimental conditions. This result mainly originated from the fact that viscosity of slag decreases with increasing basicity of the slag. Even though there are some experimental scatters in the apparent rate constant of inclusions removal with the contents of MgO and CaF_2 in the slag, the apparent rate constant seems to increase with increasing content of MgO and CaF_2. It may also be attributed to the decrease in the viscosity of the slag. However, the effect of CaF_2 greater than about 20 mass pct on the apparent rate constant is negligible. The apparent rate constant of inclusion removal decreases with increasing concentration of Al_2O_3 in the slag, which is possibly caused by an increase in the viscosity of the slag. Additionally, if the inclusion is Al_2O_3-rich, the removal rate of inclusion is strongly affected by the solubility of Al_2O_3 in the slag phase.[6–10] Hence, the composition of the inclusions was analyzed as follows.

The composition of the inclusions in molten steel at 3-minute sample was analyzed, which is plotted on the MnO-Al_2O_3-SiO_2 ternary phase diagram as shown in Figure 5. The phase diagram was computed by the FactSage^{TM}7.0 with the FToxid database at 1873 K (1600 °C) and $p(O_2) = 10^{-13}$ atm.[23–25] The composition of the inclusions is dominantly affected by the basicity (CaO/SiO_2) of slag. When the CaO/SiO_2 ratio is lower than 1.5, the composition of the inclusions is located in homogeneous liquid phase with lower melting points, whereas the composition of the inclusions is mainly positioned in the 'Al_2O_3 + Liquid' region when the CaO/SiO_2 is higher than 1.5. A difference in the inclusion types with the CaO/SiO_2 ratio should be caused by the chemical reaction between the slag and steel melt, which was discussed in previous article.[23]

Valdez et al.[9] suggested that the dissolution of the inclusion into the slag is controlled by the slag phase mass transfer and that the total dissolution time of the inclusion into the slag (τ) is given by Eq. [3].

$$\tau(s) = \frac{\rho R^2 3\pi\alpha\eta}{2kT\Delta C},$$ [3]

where ρ is the particle density, R is radius of inclusion, ΔC is the driving force for the dissolution (concentration difference), k is the Boltzmann constant, T is the temperature, α is the ionic diameter, and η is the viscosity of the slag. If the characteristics of the inclusions such as radius and composition, and the experimental conditions such as temperature are not significantly different, the total dissolution time of the inclusion can be given as Eqs. [4] and [5].

$$\tau(s) \propto \frac{\eta}{\Delta C} \propto \frac{1}{k_O}$$ [4]

$$\log k_O \propto \log \Delta C - \log \eta$$ [5]

Therefore, it is simply expected that there is a linear relationship between $\log k_O$ and $\log \Delta C - \log \eta$, which is confirmed from the measured results for the case of highly basic slags, i.e., $CaO/SiO_2 > 1.5$, as shown in Figure 6. Even though there are some experimental scatters, $\log k_O$ and $\log \Delta C - \log \eta$ exhibit a relatively good linear relationship. This result qualitatively implies that the driving force of the dissolution of the inclusion and the viscosity of the slag directly affect the removal rate of inclusion through the slag and flux layer.

REFERENCES

1. R. Kiessling and N. Lange: *Nonmetallic inclusions in steels*, The Metals Society, London, 1978, vol. III, p. 74.
2. A. Ghosh: *Secondary Steelmaking: Principles and Applications*, CRC Press, Boca Raton, 2000, p. 255.
3. M.E. Fine: *Metall. Mater. Trans. A*, 1980, vol. 11A, pp. 365–79.
4. K.H. Sandhage and G.J. Yurek: *J. Am. Ceram. Soc.*, 1988, vol. 71, pp. 478–89.
5. K.H. Sandhage and G.J. Yurek: *J. Am. Ceram. Soc.*, 1990, vol. 73, pp. 3633–42.
6. J. Choi, H.G. Lee, and J. Kim: *ISIJ Int.*, 2002, vol. 42, pp. 852–60.

7. M. Valdez, K. Prapakorn, A.W. Cramb, and S. Sridhar: *Ironmaking & Steelmaking*, 2002, vol. 29, pp. 47–53.
8. K.W. Yi, C. Tse, J. Park, M. Valdez, A.W. Cramb, and S. Sridhar: *Scand. J. Metall.*, 2003, vol. 32, pp. 177–87.
9. M. Valdez, G.S. Shannon, and S. Sridhar: *ISIJ Int.*, 2006, vol. 46, pp. 450–57.
10. S. Sridhar and A.W. Cramb: *Metall. Mater. Trans. B*, 2000, vol. 31B, pp. 406–10.
11. B.J. Monaghan and L. Chen: *Ironmak. Steelmak.*, 2006, vol. 33, pp. 323–30.
12. J.H. Park, I.H. Jung, and H.G. Lee: *ISIJ Int.*, 2006, vol. 46, pp. 1626–34.
13. S.H. Lee, C. Tse, K.W. Yi, P. Misra, V. Chevrier, C. Orrling, S. Sridhar, and A.W. Cramb: *J. Non Cryst. Solids*, 2001, vol. 282, pp. 41–48.
14. J.H. Park, J.G. Park, D.J. Min, Y.E. Lee, and Y.B. Kang: *J. Eur. Ceram. Soc.*, 2010, vol. 30, pp. 3181–86.
15. W. Yang, X. Wang, L. Zhang, Q. Shan, and X. Liu: *Steel Res. Int.*, 2013, vol. 84, pp. 473–89.
16. B.H. Reis, W.V. Bielefeldt, and A.C.F. Vilela: *ISIJ Int.*, 2014, vol. 54, pp. 1584–91.
17. J.S. Park, C. Lee, and J.H. Park: *Metall. Mater. Trans. B*, 2012, vol. 43B, pp. 1550–64.
18. J.S. Park and J.H. Park: *Steel Res. Int.*, 2014, vol. 85, pp. 1303–09.
19. S.K. Kwon, Y.M. Kong, and J.H. Park: *Met. Mater. Int.*, 2014, vol. 20, pp. 959–66.
20. S.K. Kwon and J.H. Park: *ISIJ Int.*, 2015, vol. 55, pp. 2589–96.
21. A.L. Kundu, K.M. Gupt, and P.K. Rao: *Ironmaking & Steelmaking*, 1986, vol. 13, pp. 9–15.
22. B.V. Patil and U.B. Pal: *Metall. Trans. B*, 1987, vol. 18B, pp. 583–89.
23. J.S. Park and J.H. Park: *Metall. Mater. Trans. B*, 2014, vol. 45B, pp. 953–60.
24. J.S. Park, D.H. Kim, and J.H. Park: *J. Am. Ceram. Soc.*, 2015, vol. 98, pp. 1974–81.
25. CRCT-ThermFact Inc. & GTT-Technologies. http://www.factsage.com. Accessed May 2016.